First published January 16, 2007; doi:10.1152/ajprenal.00394.2006.

COX-2 activity transiently contributes to increased water and NaCl excretion in the polyuric phase after release of ureteral obstruction

Rikke Nørregaard,[1,2] Boye L. Jensen,[4] Sukru Oguzkan Topcu,[1,2] Maria Diget,[1,2] Horst Schweer,[7] Mark A. Knepper,[5] Søren Nielsen,[1,3] and Jørgen Frøkiær[1,2,6]

[1]The Water and Salt Research Center, [2]Institute of Clinical Medicine, [3]Institute of Anatomy, University of Aarhus, [6]Department of Clinical Physiology and Nuclear Medicine, Aarhus University Hospital-Skejby, Aarhus; and [4]Department of Physiology and Pharmacology, University of Southern Denmark, Odense, Denmark; [5]Laboratory of Kidney and Electrolyte Metabolism, National Heart, Lung, and Blood Institute, National Institutes of Health, Bethesda, Maryland; and [7]Department of Pediatrics, Philipps University, Marburg, Germany

Submitted 5 October 2006; accepted in final form 12 January 2007

Nørregaard R, Jensen BL, Topcu SO, Diget M, Schweer H, Knepper MA, Nielsen S, Frøkiær J. COX-2 activity transiently contributes to increased water and NaCl excretion in the polyuric phase after release of ureteral obstruction. *Am J Physiol Renal Physiol* 292: F1322–F1333, 2007. First published January 16, 2007; doi:10.1152/ajprenal.00394.2006.—Release of bilateral ureteral obstruction (BUO) is associated with reduced expression of renal aquaporins (AQPs), polyuria, and impairment of urine-concentrating capacity. Recently, we demonstrated that 24 h of BUO is associated with increased cyclooxygenase (COX)-2 expression in the inner medulla (IM) and that selective COX-2 inhibition prevents downregulation of AQP2. In the present study, we tested the hypothesis that COX-2 activity increases in the postobstructive phase and that this increase in COX-2 activity contributes to polyuria and impaired urine-concentrating capacity. We examined the effect of the selective COX-2 inhibitor parecoxib (5 $mg \cdot kg^{-1} \cdot day^{-1}$ via osmotic minipumps) on renal functions and protein abundance of AQP2, AQP3, Na-K-2Cl cotransporter type 2 (NKCC2), and Na-K-ATPase 3 days after release of BUO. At 3 days after release of BUO, rats exhibited polyuria, dehydration and urine and IM tissue osmolality were decreased. There were inverse changes of COX-1 and COX-2 in the IM: COX-2 mRNA, protein, and activity increased, while COX-1 mRNA and protein decreased. Parecoxib reduced urine output 1 day after release of BUO, but sodium excretion and glomerular filtration rate were unchanged. Parecoxib normalized urinary PGE_2 and PGI_2 excretion and attenuated downregulation of AQP2 and AQP3, while phosphorylated AQP2 and NKCC2 remained suppressed. Parecoxib did not improve urine-concentrating capacity in response to 24 h of water deprivation. We conclude that decreased NKCC2 and collapse of the IM osmotic gradient, together with suppressed phosphorylated AQP2, are likely causes for the impaired urine-concentrating capacity and that COX-2 activity is not likely to mediate these changes in the chronic postobstructive phase after ureteral obstruction.

cyclooxygenase; ureteral obstruction; PGE_2; parecoxib; AQP2; NKCC2; urine-concentrating capacity

IT IS WELL ESTABLISHED that release of complete obstruction of the urinary tract in humans is associated with extreme polyuria and impairment of the urine-concentrating capacity (7). Sonnenberg et al. (35) demonstrated markedly lower water permeability in the medullary collecting ducts of rats subjected to postobstructive diuresis after release of 24 h of bilateral ureteral ligation. Consistent with this finding, we previously showed that release of bilateral ureteral obstruction (BUO) in rats is associated with long-term downregulation of the collecting duct water channels aquaporin (AQP)-2 and AQP3 (24). Moreover, as recently demonstrated, selective downregulation of AQP2 in postobstructed kidney may account for the higher excretion of hypotonic urine, and the local increase in PGE_2 synthesis in postobstructed kidney may be involved in AQP2 downregulation (27). Concurrently, urine-concentrating capacity in rats is impaired for ≥30 days (24). Urine-concentrating capacity depends on AVP-mediated dynamic changes in water permeability of the collecting ducts, as well as on the medullary interstitial osmotic gradient set up by the thick ascending limb of Henle's loop (TAL).

In response to 24 h of BUO, the protein expression of the Na-K-2Cl type 2 cotransporter (NKCC2), which is crucial for establishing the single effect of the osmotic gradient, is downregulated and the medullary interstitial osmolality is significantly lower than in sham-operated rats (33). Previous studies indicate that the cyclooxygenase (COX)-prostanoid pathway may contribute to renal function changes after obstruction (2, 28). It has recently been demonstrated that 24 h of BUO enhances PGE_2 production in cortical and medullary tubules of the rat kidney (37) and that PGE_2 is an established inhibitor of vasopressin-stimulated osmotic water permeability and sodium transport in collecting duct principal cells (18, 32). COX activity exerts tonic suppression of NKCC2 abundance in the TAL (10). Enhanced PGE_2 production after ureteral obstruction is mediated predominantly by COX-2. Consistent with this, we and others previously demonstrated that COX-2 expression is markedly increased in the inner medulla (IM) in response to unilateral ureteral obstruction (UUO) (3) and BUO (2, 28). Importantly, selective COX-2 inhibition attenuates downregulation of AQP2 and NKCC2 in response to BUO (28). Moreover, it was recently demonstrated that urine output in the first hours after release of obstruction is restored toward normal in rats treated with the COX-2 inhibitor NS-398 (2). These data led us to hypothesize a causal relation between increased COX-2 activity and chronic postobstructive polyuria and reduced urine-concentrating ability subsequent to BUO.

In the present study, our aims were therefore to examine *1*) whether the postobstructive-induced (3 days after release of

Address for reprint requests and other correspondence: J. Frøkiær, The Water and Salt Research Center, Institute of Clinical Medicine, Univ. of Aarhus, Dept. of Clinical Physiology and Nuclear Medicine, Aarhus Univ. Hospital-Skejby, Brendstrupgaardsvej, DK-8200 Aarhus N, Denmark (e-mail: JF@ki.au.dk).

The costs of publication of this article were defrayed in part by the payment of page charges. The article must therefore be hereby marked "*advertisement*" in accordance with 18 U.S.C. Section 1734 solely to indicate this fact.

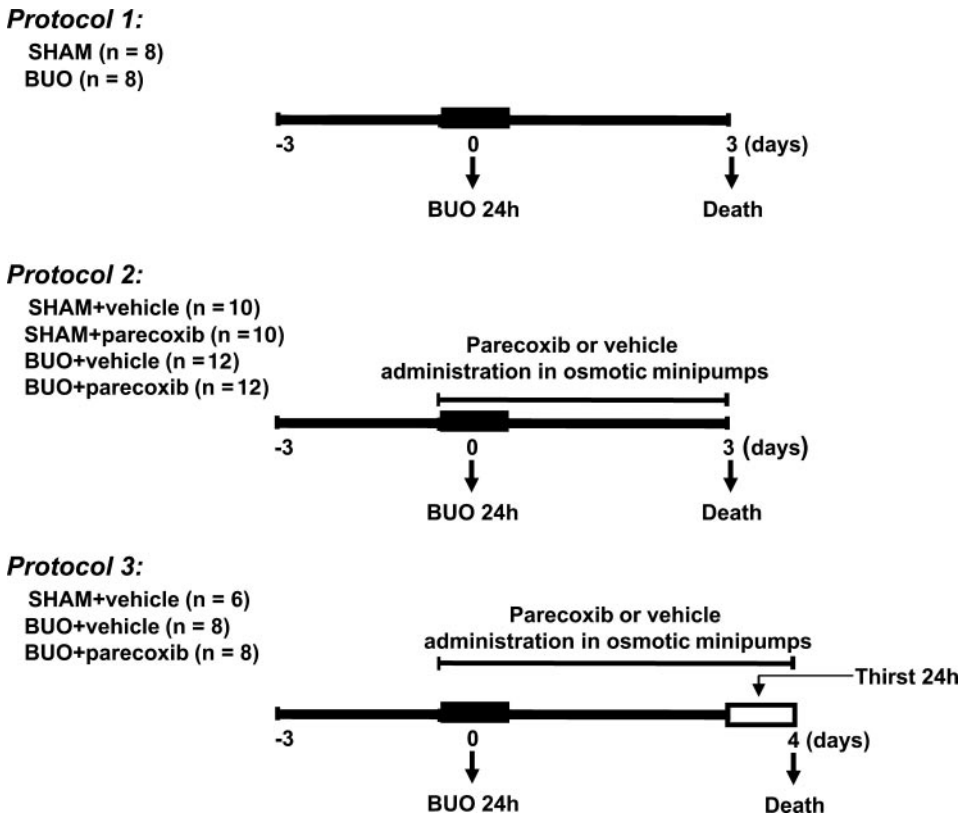

Fig. 1. Study design. *Protocol 1*: bilateral ureteral obstruction (BUO) was created and released after 24 h, and rats were monitored for the following 3 days. Sham-operated control rats matching BUO rats were also created. *Protocol 2*: BUO rats were divided into nontreated (vehicle) and parecoxib-treated (5 $mg \cdot kg^{-1} \cdot day^{-1}$ via osmotic minipumps) groups. SHAM rats were divided into nontreated (vehicle) and parecoxib-treated groups. *Protocol 3*: BUO was created and released after 24 h. Rats were monitored for the following 3 days, and then water deprived for 24 h. BUO rats were divided into nontreated (vehicle) and parecoxib-treated groups. All rats were kept in metabolic cages throughout the study. Urine was collected daily, and plasma was collected when rats were killed (Death).

BUO) natriuresis and diuresis, as well as reduced urine-concentrating capacity, in rats are associated with changes in the localization, abundance, and activity of COXs in kidney, *2*) whether selective COX-2 inhibition after release of BUO abrogates or diminishes natriuresis and diuresis and restores urine-concentrating capacity, and *3*) whether selective COX-2 inhibition attenuates downregulation of crucial transport proteins involved in the urine-concentrating capacity, i.e., Na-K-ATPase, NKCC2, AQP2, phosphorylated AQP2 (pAQP2), and AQP3.

METHODS

Experimental animals. All procedures conformed with the Danish national guidelines for the care and handling of animals and the published guidelines from the National Institutes of Health. The animal protocols were approved by the board of the Institute of Clinical Medicine of the University of Aarhus according to the licenses for use of experimental animals issued by the Danish Ministry of Justice. Male Munich-Wistar rats (250 g initial body wt; Møllegaard Breeding Centre, Eiby, Denmark) had free access to a standard rodent diet (Altromin, Lage, Germany) and tap water. During the experiments, the rats were kept in individual metabolic cages, with a 12:12-h light-dark cycle, at 21 ± 2°C and 55 ± 2% humidity. The rats were allowed to acclimatize to the cages 3–4 days before surgery. Anesthesia was induced with isoflurane (Abbott Scandinavia), and during the operation, the rats were placed on a heating pad to maintain rectal temperature at 37–38°C. Through a midline abdominal incision, both ureters were exposed, and a 5-mm-long piece of bisected polyethylene (PE-50) tubing was placed around the midportion of each ureter. The tubing was tightened with a 5-0 silk ligature to occlude the ureter. After 24 h, the obstructed ureters were decompressed by removal of the ligature and tubing.

The rats were allocated to *protocols 1–3* (see below). Age- and time-matched, sham-operated controls (SHAM) were prepared and observed in parallel with each BUO group as follows (Fig. 1).

Protocol 1. 1) BUO was induced for 24 h followed by 3 days of release ($n = 8$). Left kidneys were prepared for semiquantitative immunoblotting and right kidneys for quantitative PCR (QPCR, $n = 5$); kidneys were also prepared for immunocytochemistry ($n = 3$). *2*) SHAM rats were prepared in parallel ($n = 8$). Left kidneys were prepared for semiquantitative immunoblotting and right kidneys for QPCR ($n = 5$); kidneys were also prepared for immunocytochemistry ($n = 3$).

Protocol 2. 1) BUO was induced for 24 h followed by 3 days of release. In *group 1*, osmotic minipumps (Alzet, Scanbur, Denmark) containing saline were surgically implanted subcutaneously ($n = 12$). In *group 2*, osmotic minipumps containing parecoxib (Dynastat, Pfizer, Ballerup, Denmark) dissolved in saline (40 mg/ml) were surgically implanted subcutaneously when the obstruction was performed, and parecoxib was administered at 5 $mg \cdot kg^{-1} \cdot day^{-1}$ throughout the treatment period ($n = 12$). *2*) SHAM rats were subjected to a similar surgical procedure without ureteral occlusion. In *group 3*, osmotic minipumps containing saline were implanted subcutaneously ($n = 10$). In *group 4*, osmotic minipumps containing parecoxib dissolved in saline (40 mg/ml) were surgically implanted subcutaneously, and parecoxib was administered at 5 $mg \cdot kg^{-1} \cdot day^{-1}$ throughout the control period ($n = 10$). Administration of parecoxib at 5 $mg \cdot kg^{-1} \cdot day^{-1}$ was based on a previously demonstrated pharmacological profile of parecoxib (30). Left kidneys were prepared for semiquantitative immunoblotting and QPCR and right kidneys for measurements of IM osmolality in the BUO ($n = 8$) and SHAM ($n = 6$) rats; kidneys were also prepared for immunocytochemistry ($n = 4$).

Protocol 3. 1) BUO was induced for 24 h followed by 3 days of release. Urine-concentrating capacity in response to 24 h of water

deprivation was examined 3–4 days after release of BUO. In *group 1*, saline-containing osmotic minipumps were surgically implanted subcutaneously ($n = 8$). In *group 2*, osmotic minipumps containing parecoxib dissolved in saline (40 mg/ml) were surgically implanted subcutaneously when the obstruction was performed, and parecoxib was administered at 5 $mg \cdot kg^{-1} \cdot day^{-1}$ throughout the treatment period ($n = 8$). *2*) SHAM rats were operated in parallel. In *group 3*, osmotic minipumps containing saline were implanted subcutaneously ($n = 6$).

Clearance studies. Urine was collected over 24-h period in *protocols 2* and *3,* and clearance studies were performed during the last 24 h in each protocol. The rats were reanesthetized with isoflurane at the end of each protocol. Before each rat was killed, the aortic bifurcation was localized and dissected free, and a 5- to 7-ml blood sample was collected for determination of plasma electrolytes and osmolality. The kidneys were rapidly removed, and the IM was dissected and frozen in liquid nitrogen. The plasma and urine concentrations of creatinine and urea were measured (Vitros 950, Johnson & Johnson). Finally, osmolality of the plasma and urine was determined with a vapor pressure osmometer (Osmomat 030, Gonotec, Berlin, Germany).

Measurement of IM osmolality. Tissue was processed by a modification of the method described by Schmidt-Nielsen et al. (33). Briefly, kidneys were removed, and individual IMs were rapidly excised, snapfrozen in liquid nitrogen and stored at −80°C. During the analysis, the IMs were placed in preweighed tubes. Samples were weighed immediately and subsequently dried over a desiccant at 60°C

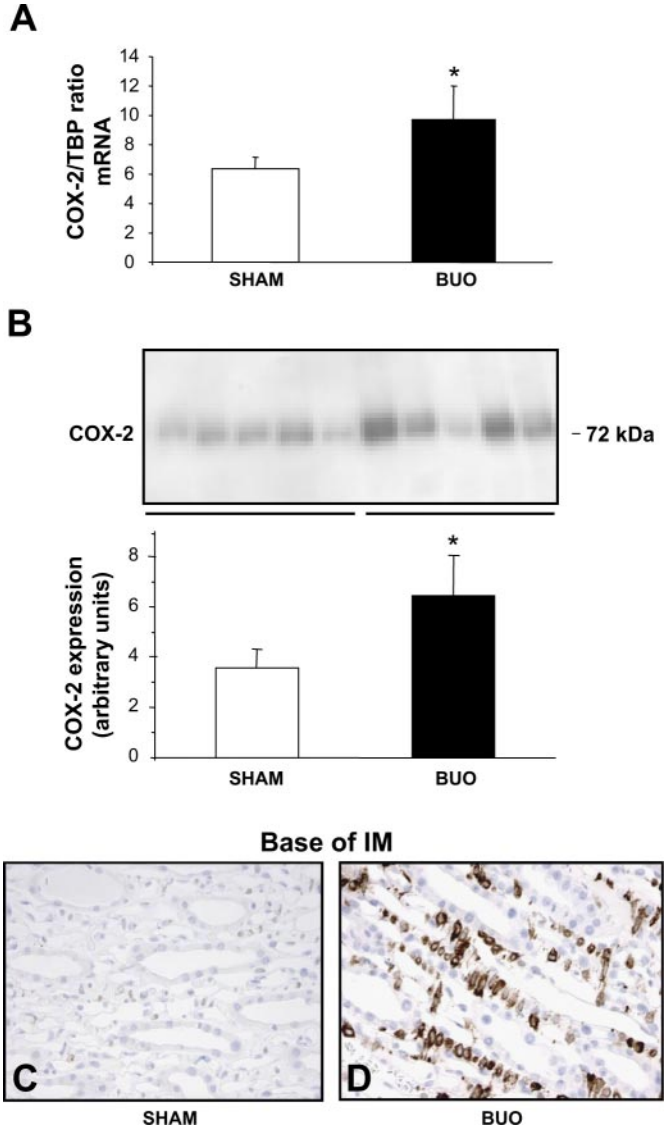

Fig. 2. Expression of cyclooxygenase (COX)-2 mRNA and protein in the inner medulla (IM) from SHAM and BUO rats. *A*: representative quantitative PCR (QPCR) for COX-2 and TATA box-binding protein (TBP). For QPCR, 100 ng of cDNA were used. Values are means ± SE. $*P < 0.05$ BUO vs. SHAM. *B*: immunoblot reacted with anti-COX-2 antibody. Note 2 discernible bands (72 and 74-kDa). A total of 20 μg of protein were used for COX-2 assay. Densitometric analyses of all samples revealed an increase of COX-2 protein in BUO rats compared with SHAM rats. Values are means ± SE. $*P < 0.05$ BUO vs. SHAM. *C* and *D*: immunohistochemistry for COX-2 at the base of the IM of SHAM and BUO rats. COX-2 immunoreactivity was detected in interstitial cells, and labeling was much stronger in BUO than in SHAM rats.

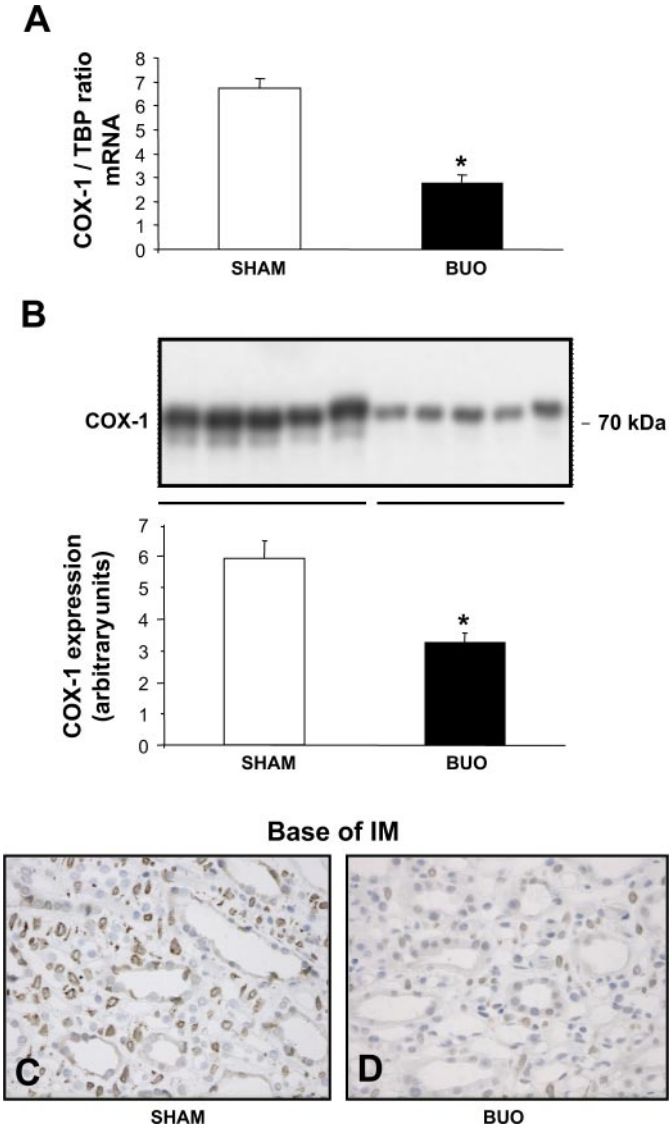

Fig. 3. COX-1 mRNA and protein expression in the IM of SHAM and BUO rats. *A*: representative QPCR for COX-1 and TBP. For QPCR, 100 ng of cDNA were used. Values are means ± SE. $*P < 0.05$ BUO vs. SHAM. *B*: immunoblot reacted with anti-COX-1 antibody. Note 71-kDa band. A total of 20 μg protein were used for COX-1 assay. Densitometric analyses of all samples revealed a decrease of COX-1 protein level in BUO rats compared with SHAM rats. Values are means ± SE. $*P < 0.05$ BUO vs. SHAM. *C* and *D*: immunohistochemistry for COX-1 at the base of the IM of SHAM and BUO rats. COX-1 immunoreactivity was detected in interstitial cells and collecting ducts, and labeling was much weaker in BUO than in SHAM rats.

Table 1. *GFR, urine, and plasma biochemical values: protocol 2*

	SHAM + Vehicle (n = 6)	SHAM + Parecoxib (n = 6)	BUO + Vehicle (n = 8)	BUO + Parecoxib (n = 8)
GFR, $\mu l \cdot min^{-1} \cdot kg^{-1}$	9.5±0.5	7.8±0.8	3.4±0.5*	4.2±0.8*
T^cH_2O, $\mu l \cdot min^{-1} \cdot kg^{-1}$	175±15.5	146±17.3	86.1±5.7*	61.8±9.9*
P_{osmol}, mosmol/kgH_2O	300±1.2	302±2.3	313±5.2*	327±13*
P_{urea}, mM	6.4±0.3	6.1±0.3	12.6±3.4*	10.3±1.9*
U_{urea}, mM	1,269±162	1,172±122	460±51*	410±42*

Values are means ± SE; *n,* number of rats. SHAM, sham-operated control rats; BUO, bilateral ureteral obstruction; GFR, glomerular filtration rate; T^cH_2O solute-free water reabsorption; P_{osmol}, plasma osmolality; P_{urea}, plasma urea concentration; U_{urea}, urine urea concentration. *$P < 0.05$ BUO vs. SHAM.

for 2.5 h (after which weight remained constant). After the samples were reweighed, 150 μl of distilled water were added to each tube. The tubes were capped, kept at 95°C for 30 min, and, after brief centrifugation, stored at 4°C for 24 h for diffusion. After centrifugation for 1 min at 8,000 *g*, supernatant osmolality was determined with a vapor pressure osmometer (Osmomat 030, Gonotec).

Measurement of urinary prostanoid excretion before and after release of obstruction. In an isotope-dilution assay, PGE_2 and the PGI_2 metabolite 6-keto-$PGF_{1\alpha}$ were determined in urine by gas chromatography-tandem mass spectrometry (GC-MS-MS). After addition of deuterated internal standards, the prostanoids were derivatized to methoximes and extracted with ethyl acetate-hexane. The samples were further derivatized to the pentafluorobenzyl esters and purified using TLC. Three zones were scraped from the TLC. The prostanoid derivatives were converted to the trimethylsilyl ethers, and the products were quantified using GC-MS-MS.

GC-MS-MS analysis. A GC-MS-MS (model MAT TSQ700, Finnigan) equipped with a gas chromatograph (Varian 3400) and an autosampler (model CTC A200S) was used. Gas chromatography of prostanoid derivatives was carried out on a DB-1 (20-m, 0.25-mm ID, 0.25-μm film thickness) capillary column (Analyt, Mühlheim, Germany) in the splitless mode. GC-MS-MS parameters were exactly as described by Schweer et al. (34).

QPCR. For QPCR, 100 ng of cDNA served as a template for PCR amplification using Brilliant SYBR Green QPCR Master Mix according to the manufacturer's instruction (Stratagene). Serial dilution (1 ng–1 fg/μl) of cDNA was used as template for generation of a standard curve. Nested primers were used to amplify standards and kidney cDNA samples as follows: GGA ATT CAA CCA CCT CTA TCA CTG (sense) and GAC ACC GTA GTC CAC CAG CAT A (antisense) for COX-1 (GenBank accession no. NM_017043, 121 bp), CCT TGA AGA CGG ACT TGC TCA C (sense) and TCT CTC TGC TCT GGT CAA TGG A (antisense) for COX-2 (GenBank accession no. U03389, 131 bp), ACC AAG AAC CTC CCT CCT GT (sense) and TCG GAC ACC AAG GTA CAA CA (antisense) for NKCC2 (GenBank accession no. NM_019134, 107 bp), and GAC TCC TGT CTC CCC TAC CC (sense) and CTC AGT GCA GAG GAG GGA AC (antisense) for TATA box-binding protein (TBP; GenBank accession no. NM_001004198, 162 bp). Standards and unknown samples were amplified in duplicate in 96-well plates, and PCR was performed for 50 cycles, consisting of denaturation for 30 s at 95°C followed by annealing and polymerization at 60°C for 1 min. Emitted fluorescence was detected during the annealing/extension step in each cycle. Specificity was ensured by postrun melting curve analysis.

Membrane fractionation for immunoblotting. Tissue from the IM was homogenized in dissecting buffer [0.3 M sucrose, 25 mM imidazole, 1 mM EDTA (pH 7.2), and the protease inhibitors 8.5 μM leupeptin (a serine and cysteine protease inhibitor; Sigma-Aldrich) and 0.4 mM Pefabloc (a serine protease inhibitor; Roche)]. Moreover dissecting buffer for the IM was added after addition of the phosphatase inhibitors sodium orthovanadate (Sigma-Aldrich), NaF (Merck), and okadaic acid (Calbiochem). The tissue was homogenized for 30 s at 1,250 rpm (Ultra-Turrax T8 homogenizer, IKA Labortechnik) and then centrifuged at 4,500 *g* at 4°C for 15 min. Gel samples were prepared from the supernatant in Laemmli sample buffer containing 2% SDS. For COX-1 and COX-2, homogenates were homogenized for 30 s at 1,250 rpm (Ultra-Turrax T8 homogenizer) in dissecting buffer and then centrifuged at 10,000 *g* for 10 min. The supernatant was centrifuged for 60 min at 100,000 *g* to sediment microsomes, as described previously (15). The microsomes were resuspended in dissecting buffer, mixed with an equal volume of 2× SDS sample buffer, and boiled for 5 min. Total protein concentration of the homogenate was measured using a Pierce bicinchoninic acid protein assay kit (Roche).

Electrophoresis and immunoblotting. Samples of membrane fractionation from the IM were run on a 12% polyacrylamide minigel

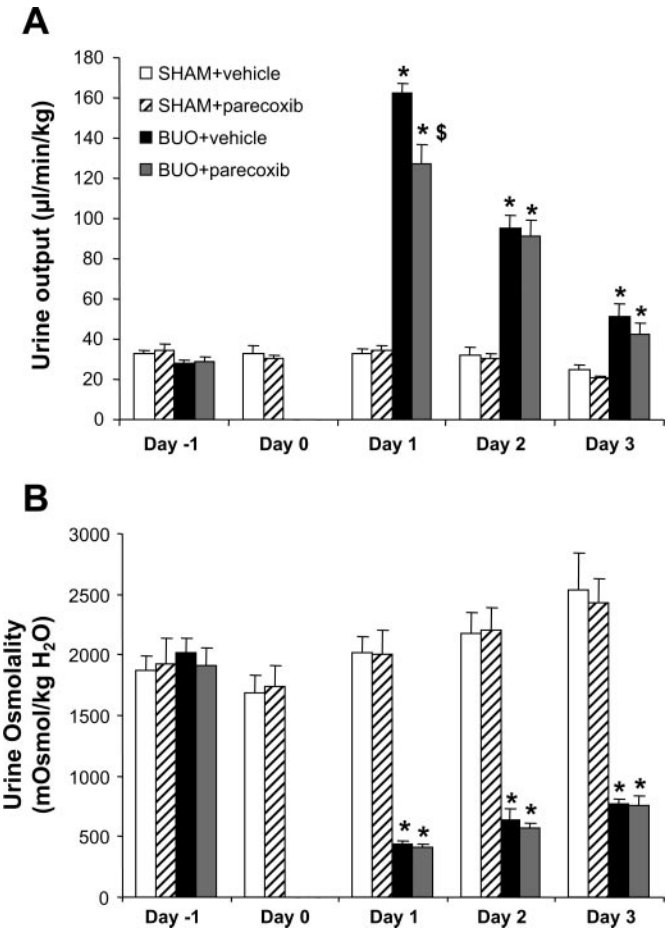

Fig. 4. Urine output and osmolality in parecoxib-treated and untreated (vehicle) BUO rats compared with SHAM rats in *protocol 2*. Values are means ± SE (n = 6 SHAM and 8 BUO). *$P < 0.05$ BUO vs. SHAM. $ $P < 0.05$ BUO + parecoxib vs. BUO + vehicle.

Table 2. *Changes in renal sodium excretion after release of BUO: protocol 2*

	SHAM + Vehicle (n = 6)	SHAM + Parecoxib (n = 6)	BUO + Vehicle (n = 8)	BUO + Parecoxib (n = 8)
Na^+ excretion, $\mu mol \cdot min^{-1} \cdot kg^{-1}$				
Day − 1	4.2±0.2	4.7±0.4	3.7±0.1	3.7±0.2
Day 1	5.8±0.4	6.1±0.4	11.1±1.7*	9.1±1.1*
Day 3	4.6±0.4	3.8±0.4	1.7±0.4*	1.6±0.5*
Fl_{Na}^+, $\mu mol \cdot min^{-1} \cdot kg^{-1}$	1,328±67	1,087±118	478±60*	584±117*
Net Na reabsorption, $\mu mol \cdot min^{-1} \cdot kg^{-1}$	1,323±66	1,084±118	476±61*	582±116*

Values are means ± SE; *n,* number of rats. FL_{Na}^+, filtered load of sodium. *$P < 0.05$ BUO vs. SHAM.

(Mini Protean II, Bio-Rad). For each gel, an identical gel was run in parallel and subjected to Coomassie staining. The Coomassie-stained gel was used to determine identical loading or to allow for correction for minor variations in loading.

Samples were run on 9 and 12% polyacrylamide gels (Mini Protean II, Bio-Rad). Proteins were transferred to a nitrocellulose membrane (Hybond ECL RPN 3032D, Amersham Pharmacia Biotech). The blots were blocked with 5% nonfat dry milk in PBS-T (80 mM Na_2HPO_4, 20 mM NaH_2PO_4, 100 mM NaCl, and 0.1 Tween 20, adjusted to pH 7.4). After they were washed with PBS-T, the blots were incubated with primary antibodies overnight at 4°C. Antigen-antibody complex was visualized with horseradish peroxidase-conjugated secondary antibodies (diluted 1:3,000; catalog no. P448, Dako, Glostrup, Denmark) using an enhanced chemiluminiscence system (ECL, Amersham Pharmacia Biotech). For immunolabeling controls, peptide-absorbed antibody was used.

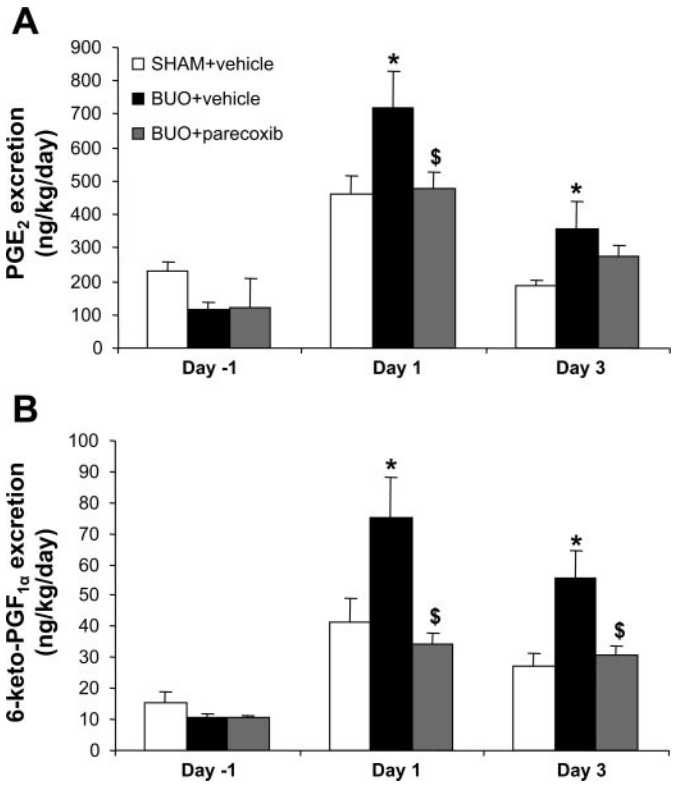

Fig. 5. Effect of parecoxib on urinary excretion of PGE_2 and the PGI_2 metabolite 6-keto-$PGF_{1\alpha}$. BUO was induced for 24 h followed by 3 days of release. Parecoxib (5 $mg \cdot kg^{-1} \cdot day^{-1}$) or saline was administrated in osmotic minipumps during obstructed and release periods. PGE_2 and 6-keto-$PGF_{1\alpha}$ were measured before obstruction (*day −1*) and on 1 and 3 days after release. Values are means ± SE (n = 6 SHAM and 8 BUO). *$P < 0.05$ BUO vs. SHAM. $ $P < 0.05$ BUO + parecoxib vs. BUO + vehicle.

Primary antibodies. For semiquantitative immunoblotting and immunocytochemistry, we used previously characterized monoclonal and polyclonal antibodies as follows: an affinity-purified rabbit polyclonal antibody against COX-1 (catalog no. 160109, Cayman Chemical, Ann Arbor, MI); an affinity-purified rabbit polyclonal antibody against COX-2 (catalog no. 160126, Cayman Chemical); an immune serum or an affinity-purified antibody to AQP2 (LL127 serum or LL127AP), as previously described (6); an affinity-purified rabbit polyclonal antibody to pAQP2 (AN224-pp-AP), as previously described (4); an affinity-purified polyclonal antibody to AQP3 (LL178AP), as previously described (8); a monoclonal antibody against the α_1-subunit of Na-K-ATPase, as previously described (21); and an affinity-purified polyclonal antibody to the apical Na-K-2Cl cotransporter of the TAL (LL320AP), as previously described (9).

Immunocytochemistry. The kidneys from BUO and SHAM rats were fixed by retrograde perfusion via the abdominal aorta with 3% paraformaldehyde in 0.1 M cacodylate buffer (pH 7.4). Moreover, the kidneys were immersion fixed for 1 h and washed three times for 10 min each with 0.1 M cacodylate buffer. The kidney blocks were dehydrated and embedded in paraffin. The paraffin-embedded tissues were cut into 2-μm sections on a rotary microtome (Leica Microsystems, Herlev, Denmark).

For immunoperoxidase labeling, the sections were deparaffinated and rehydrated. Endogenous peroxidase activity was blocked with 5% H_2O_2 in absolute methanol for 10 min at room temperature. For exposure of antigens, kidney sections were boiled in a target retrieval solution [1 mmol/l Tris (pH 9.0) with 0.5 mM EGTA] for 10 min. After the sections were cooled, they were incubated in 50 mM NH_4Cl in PBS for 30 min to prevent nonspecific binding and then blocked in PBS containing 1% BSA, 0.05% saponin, and 0.2% gelatin. Sections were incubated with primary antibodies diluted in PBS with 0.1% BSA and 0.3% Triton X-100 overnight at 4°C. After they were washed three times for 10 min each with PBS supplemented with 0.1% BSA, 0.05% saponin, and 0.2% gelatin, the sections were incubated with horseradish peroxidase-conjugated secondary antibody (catalog no. P448, goat anti-rabbit immunoglobulin, Dako) for 1 h at room temperature. After the sections were rinsed with PBS wash buffer, the sites of antibody-antigen reactions were visualized with 0.05% 3,3′-diaminobenzidine tetrachloride (Kem-en Tek, Copenhagen, Denmark) dissolved in distilled water with 0.1% H_2O_2. The

Table 3. *GFR and urine and plasma biochemical values: protocol 3*

	SHAM + Vehicle (n = 6)	BUO + Vehicle (n = 8)	BUO + Parecoxib (n = 8)
GFR, μl/min/kg	6.7±0.5	4.5±0.6*	3.7±0.6*
T^cH_2O, μl/min/kg	128±10.1	110.5±8.9	99.2±19.8
P_{osmol}, mosmol/kgH_2O	314±1.3	323±2.6*	334±6.2*
P_{urea}, mM	8.6±0.5	8.8±1.1	13.4±4.4
U_{urea}, mM	1,904±218	946±111*	869±102*

Values are means ± SE; *n,* number of rats. *$P < 0.05$ BUO vs. SHAM.

sections were observed under a light microscope (model DMRE, Leica Microsystem).

Statistics. Values are means ± SE. Statistical comparisons between experimental groups were made by a standard unpaired *t*-test or one-way ANOVA with Bonferroni's correction. $P < 0.05$ was considered significant.

RESULTS

Increased renal IM COX-2 expression after release of 24-h BUO. The abundance of COX-2 mRNA normalized for TBP was significantly increased 1.5-fold in the BUO rats compared with the SHAM rats (Fig. 2*A*). Semiquantitative immunoblotting showed that BUO followed by 3 days of release significantly induced COX-2 ($P < 0.05$; Fig. 2*B*). Immunohistochemistry revealed localization of COX-2 protein in the medullary interstitial cells and there was a marked increase in COX-2 labeling of the interstitial cells at the base of the IM in BUO rats (Fig. 2*D*) compared with SHAM rats (Fig. 2*C*).

COX-1 mRNA normalized for TBP decreased significantly in the IM of BUO rats compared with SHAM rats (Fig. 3*A*). In accordance, the protein expression of COX-1 was reduced in the IM in BUO rats compared with SHAM rats ($P < 0.01$; Fig. 3*B*). Consistent with the reduced mRNA and protein expression, immunohistochemical analysis of COX-1 protein demonstrated a marked reduction in labeling of the collecting ducts and the interstitial cells at the base of the IM in BUO rats compared with SHAM rats (Fig. 3, *C* and *D*).

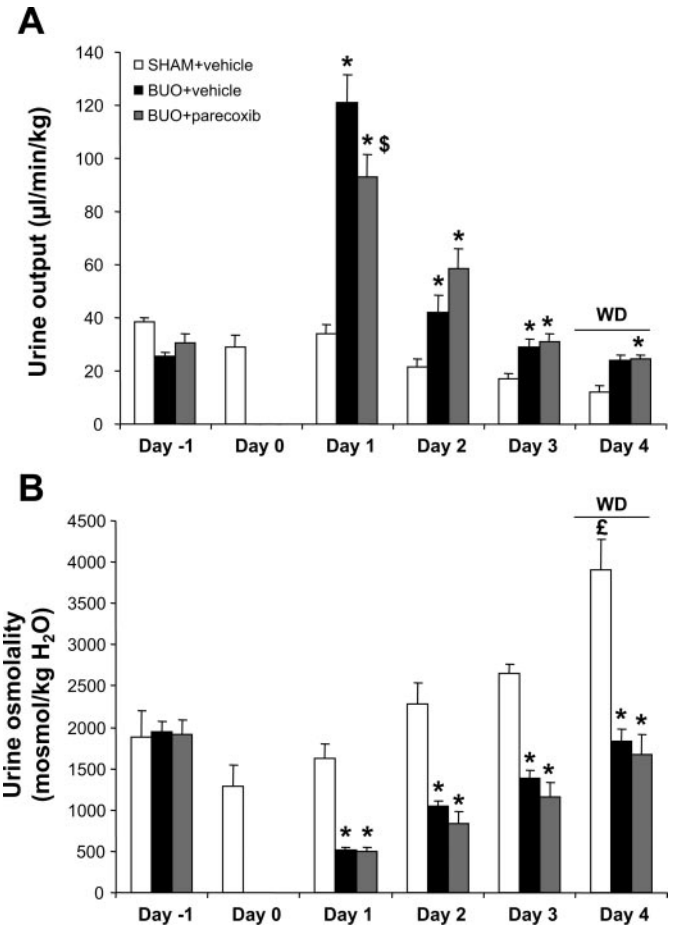

Fig. 6. Urine output and osmolality in parecoxib-treated and untreated BUO rats compared with matched SHAM rats in *protocol 3*. Values are means ± SE ($n = 6$ SHAM and 8 BUO). WD, water deprivation. *$P < 0.05$ BUO vs. SHAM. $ $P < 0.05$ BUO + parecoxib vs. BUO + vehicle. £ $P < 0.05$ SHAM + vehicle on *day 4* vs. SHAM + vehicle on *days −1, 0, 1, 2*, and *3*.

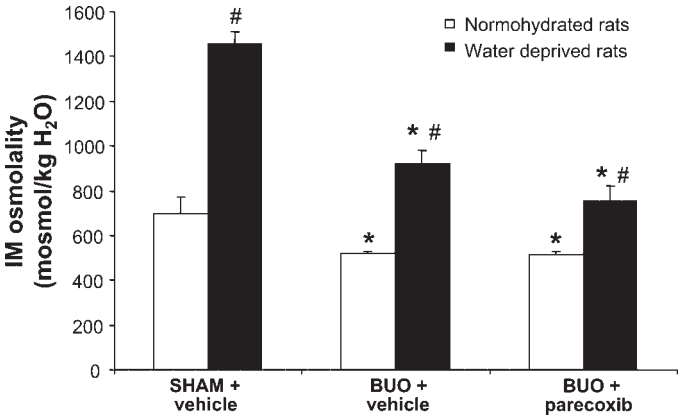

Fig. 7. IM osmolality in parecoxib-treated and untreated BUO and SHAM rats in *protocols 2* and *3*. Values are means ± SE ($n = 6$). *$P < 0.05$ BUO vs. SHAM. # $P < 0.05$ water-deprived rats vs. normohydrated rats.

Effect of COX-2 inhibition on BUO-mediated changes in glomerular filtration rate, diuresis, and plasma and urine electrolytes 3 days after BUO release. In *protocol 2*, the effect of the selective COX-2 inhibitor parecoxib (5 $mg \cdot kg^{-1} \cdot day^{-1}$) on renal function parameters and transport proteins was examined before and 3 days after release of BUO.

Glomerular filtration rate (GFR) and solute-free water reabsorption were significantly reduced in BUO rats compared with SHAM rats (Table 1). Plasma osmolality and urea were elevated 3 days after release of BUO, while urinary urea concentration was reduced (Table 1). Thus BUO rats were dehydrated 3 days after obstruction was released. Parecoxib did not affect these parameters in the SHAM or BUO rats (Table 1). Urine output did not differ between vehicle- and parecoxib-treated SHAM rats over the 5 study days (Fig. 4*A*). In marked contrast, urine output increased fivefold 1 day after release of obstruction and then slowly recovered in BUO vehicle-treated rats, but urine output remained significantly higher 3 days after release of BUO than in control rats (Fig. 4*A*). Parecoxib significantly lowered urine output 1 day after release of BUO but had no significant effect 2 and 3 days after release of obstruction (Fig. 4*A*). Sodium excretion displayed a biphasic change: it increased markedly 1 day after release of obstruction, whereas 3 days after release of BUO it was significantly lower than in SHAM rats (Table 2). The filtered load of sodium and net reabsorption of sodium were lower 3 days after release of BUO (Table 2). Parecoxib did not change sodium excretion after release of obstruction (Table 2).

There was no significant difference between the untreated and treated SHAM rats with regard to urine osmolality (Fig. 4*B*). In contrast, urine osmolality decreased fivefold 1 day after release of obstruction and then recovered significantly 2 and 3 days after release (Fig. 4*B*). Urine osmolality was significantly lower 3 days after release of BUO than in SHAM rats, and inhibition of COX-2 did not alter these changes in urine osmolality after release of obstruction (Fig. 4*B*). Renal IM tissue interstitial osmolality was determined in *protocol 2* (3 days after release of the obstruction). Interstitial osmolality

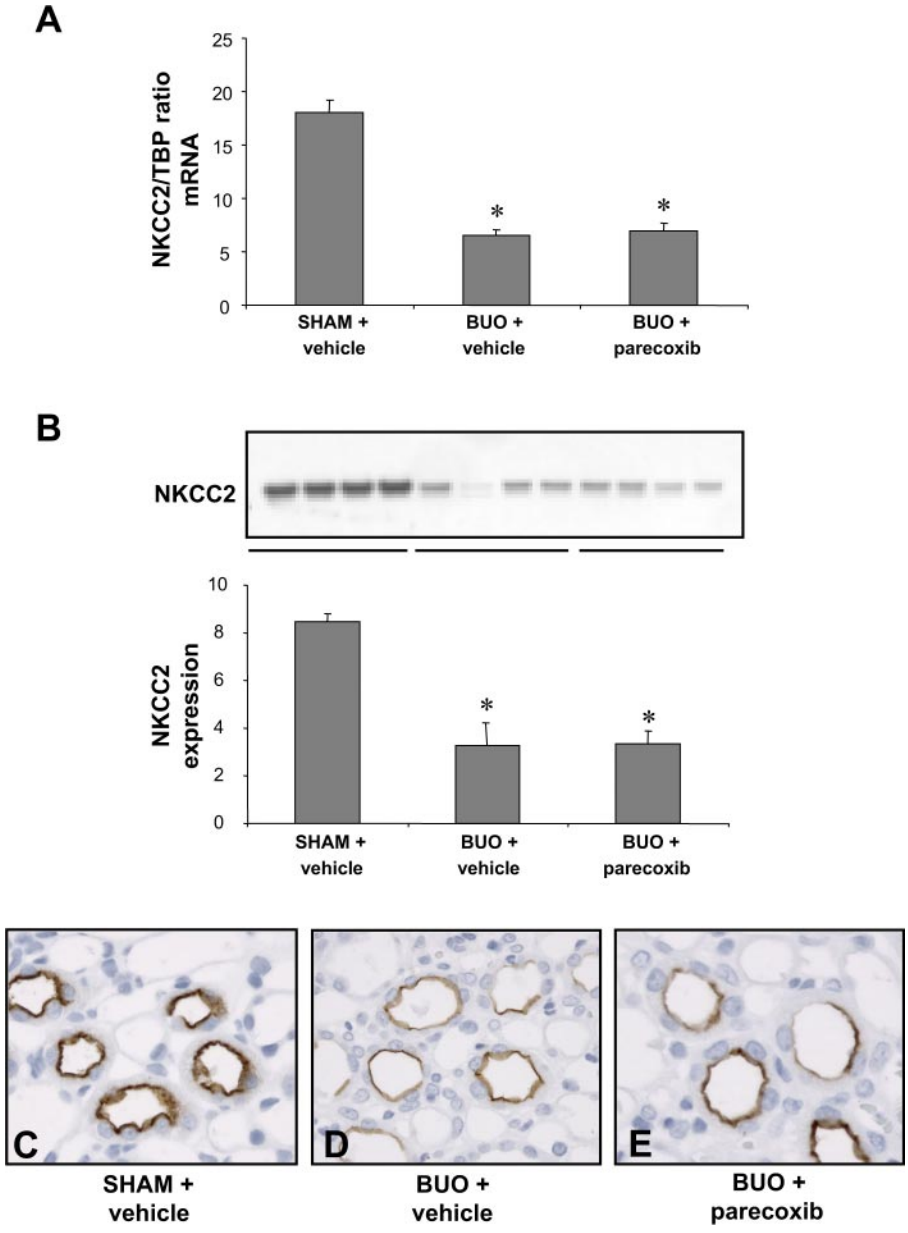

Fig. 8. Na-K-2Cl type 2 cotransporter (NKCC2) mRNA and protein expression in the outer medulla (OM) of SHAM and BUO parecoxib-treated and untreated rats. *A*: representative QPCR for NKCC2 and TBP. For QPCR, 100 ng of cDNA were used. NKCC2 mRNA was downregulated in BUO rats compared with SHAM rats. Parecoxib did not attenuate the reduced NKCC2 mRNA in BUO rats. Values are means ± SE. $*P < 0.05$ BUO vs. SHAM. *B*: immunoblot reacted with anti-NKCC2 antibody. Note band at ~161 kDa. Densitometric analyses revealed marked decrease in NKCC2 expression in the OM of BUO rats compared with SHAM rats. Parecoxib did not prevent this decrease in NKCC2 expression in BUO rats. Values are means ± SE. $*P < 0.05$ BUO vs. SHAM. *C–E*: immunohistochemistry for NKCC2 in kidney medulla of SHAM, untreated BUO, and parecoxib-treated BUO rats. Immunoperoxidase microscopy demonstrated association of NKCC2 labeling with apical membrane of the thick ascending limb of Henle's loop (TAL) in the OM of SHAM rats (*C*). NKCC2 labeling was reduced in BUO rats (*D*). Parecoxib did not change labeling intensity of NKCC2 in BUO rats (*E*).

was significantly lower than urine osmolality in all samples and was lower in BUO than in SHAM rats (see Fig. 6). Administration of parecoxib before, during, and after release of obstruction did not change interstitial osmolality (see Fig. 6).

Effect of COX-2 inhibition on urinary prostanoid excretion after release of obstruction. To validate inhibition of COX-2 in the kidney, we examined the effect of parecoxib on urinary excretion of PGE_2 and the PGI_2 metabolite 6-keto-$PGF_{1\alpha}$ in *protocol 2*. Urinary excretion of the two prostanoids increased significantly 1 and 3 days after release of BUO compared with SHAM rats (Fig. 5). The increase in urinary PGE_2 (Fig. 5*A*) and 6-keto-$PGF_{1\alpha}$ excretion (Fig. 5*B*) was abolished by parecoxib 1 day after release of BUO. At 3 days after release of obstruction, COX-2 inhibition significantly lowered urinary excretion of the PGI_2 metabolite 6-keto-$PGF_{1\alpha}$.

Effect of COX-2 inhibition and water deprivation on BUO-mediated changes in renal function after release of obstruction. To test whether urine-concentrating capacity was lowered by COX-2 activity 3 days after release of BUO, rats were challenged by 24 h of water deprivation in *protocol 3* (Fig. 1). Vehicle-treated SHAM rats and parecoxib-treated and untreated BUO rats were subjected to water deprivation. At 1–3

Table 4. *Summary of densitometry of immunoblots of Na-K-ATPase: protocol 2*

	SHAM + Vehicle ($n = 6$)	BUO + Vehicle ($n = 6$)	BUO + Parecoxib ($n = 6$)
Outer medulla	4.5±0.3	3.7±0.4	4.4±0.5
Inner medulla	5.5±1.1	1.5±0.4*	3.4±1.0

Values are means ± SE. $*P < 0.05$ BUO vs. SHAM.

days after release of BUO before water deprivation, GFR, plasma osmolality, diuresis, and urine osmolality changed, as observed in *protocol 2* (Table 3, Fig. 6). Similar to the results of *protocol 2*, COX-2 inhibition decreased urine output significantly 1 day after release of obstruction but had no effect 2 and 3 days after BUO. However, urine output was higher after release of BUO than in SHAM rats, consistent with impaired urine-concentrating capacity in the BUO rats (Fig. 6*A*). In the BUO rats, COX-2 inhibition by parecoxib did not significantly change urine output and urine osmolality after water deprivation (Fig. 6). However, 24 h of water deprivation led to an increase in urine osmolality in the SHAM rats compared with urinary osmolality at *day 3* (Fig. 6*B*).

In vehicle-infused SHAM rats, IM tissue osmolality increased significantly during water deprivation compared with normal hydration (Fig. 7). IM tissue osmolality also increased in the water-deprived BUO rats compared with the normally hydrated BUO rats but was significantly lower than in the water-deprived SHAM rats (Fig. 7). COX-2 inhibition did not increase IM tissue osmolality compared with vehicle-infused water-deprived BUO rats (Fig. 7). Thus urine-concentrating capacity was impaired 3 days after release of BUO and was not improved by parecoxib treatment. IM interstitial osmolality was lower than urine osmolality in all tested samples (Figs. 6 and 7).

Effect of COX-2 inhibition on changes in NaCl transporters and AQPs after release of BUO. We determined the abundance of NaCl transporters with a key role in TAL function and urine-concentrating ability, NKCC2 and Na-K-ATPase.

NKCC2 mRNA normalized for TBP in the outer medulla (OM) was significantly downregulated in the BUO rats compared with the SHAM rats (Fig. 8*A*). Immunoblotting of renal OM membrane fractions of BUO and SHAM rats revealed marked suppression of NKCC2 abundance 3 days after release of BUO (Fig. 8*B*). This downregulation at the mRNA and the protein level was resistant to COX-2 inhibition (Fig. 8, *A* and *B*). Immunohistochemistry revealed that labeling of NKCC2 was localized to the apical plasma membrane of the TAL cells in the OM (Fig. 8*C*). In the obstructed kidney, NKCC2 labeling was significantly weaker (Fig. 8*D*). Consistent with immunoblotting and QPCR, there was no apparent difference in the labeling density of NKCC2 between the parecoxib-treated and untreated BUO rats (Fig. 8*E*).

The abundance of Na-K-ATPase appeared more robust and did not change in the OM after release of BUO (Table 4), but Na-K-ATPase abundance decreased in the IM (Table 4).

AQP2 and AQP3 protein abundance was reduced significantly 3 days after release of BUO compared with SHAM rats ($P < 0.01$; Figs. 9*A* and 10*A*). Parecoxib significantly attenuated the BUO-induced reduction in AQP2 and AQP3 expres-

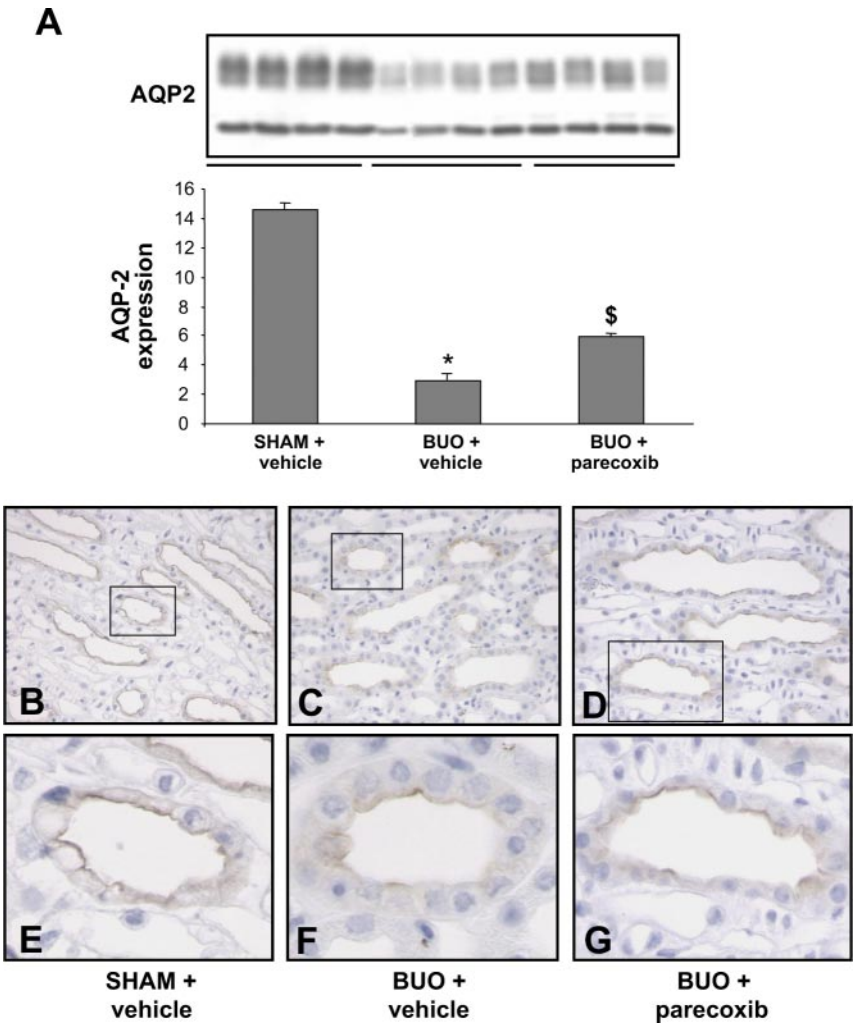

Fig. 9. Semiquantitative immunoblot of aquaporin (AQP)-2 in protein isolated from the IM of SHAM, BUO, and parecoxib-treated BUO rats. *A*: immunoblot reacted with affinity-purified anti-AQP2 antibody. Note 29- and 35- to 50-kDa bands representing nonglycosylated and glycosylated forms of AQP2. Densitometric analyses revealed marked decrease in AQP2 expression in the IM of BUO rats compared with SHAM rats. Parecoxib partly prevented this decrease in AQP2 expression in BUO rats. *$P < 0.05$ BUO vs. SHAM. \$ $P < 0.05$ BUO + parecoxib vs. BUO + vehicle. *B–G*: immunohistochemistry for AQP2 in the IM of SHAM, untreated BUO, and parecoxib-treated BUO rats. Immunoperoxidase microscopy demonstrated association of AQP2 labeling with apical plasma membrane of principal cells in collecting ducts in the IM of SHAM rats (*B* and *E*). Labeling of AQP2 was reduced in untreated BUO rats (*C* and *F*). Labeling in parecoxib-treated BUO rats was almost comparable to that in SHAM rats (*D* and *G*).

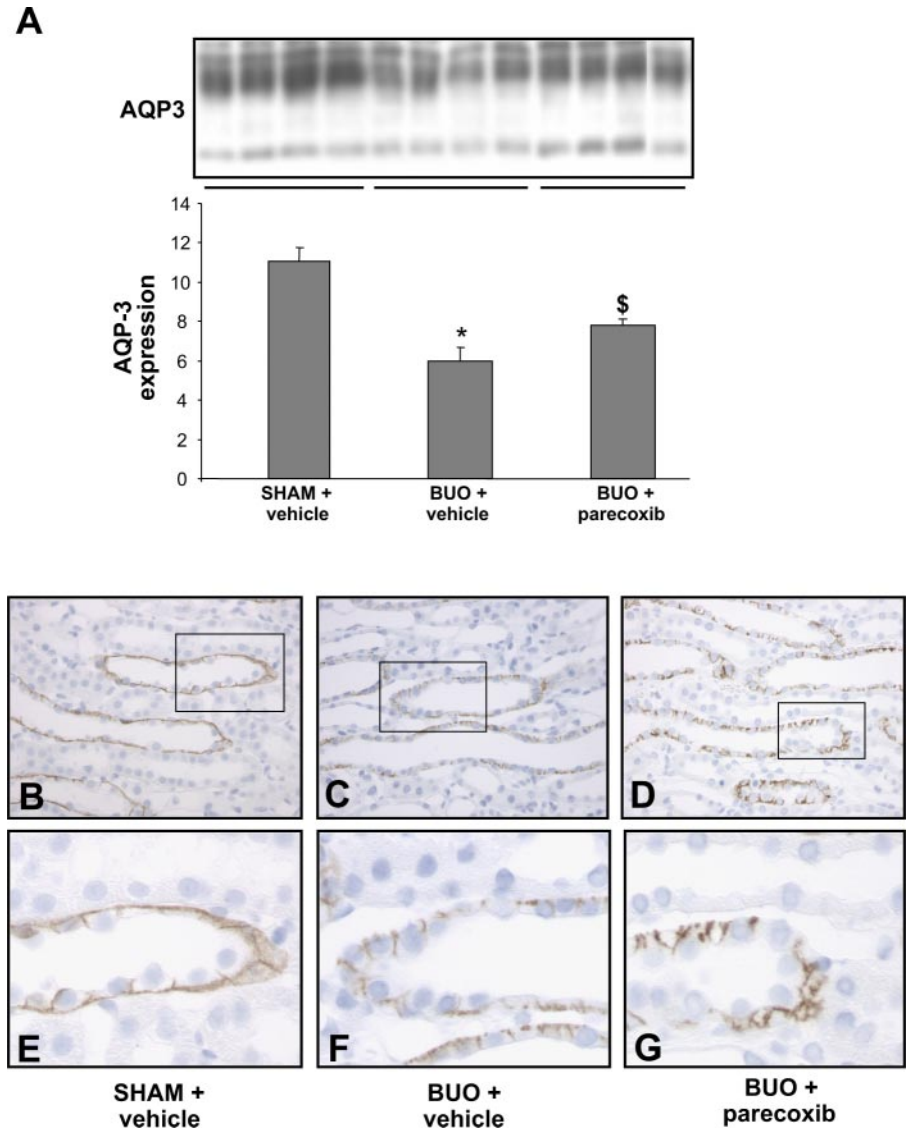

Fig. 10. Semiquantitative immunoblot of AQP3 in protein isolated from the IM of SHAM, untreated BUO, and parecoxib-treated BUO rats. *A*: immunoblot reacted with affinity-purified anti-AQP3 antibody. Note 27- and 33- to 40-kDa bands, representing nonglycosylated and glycosylated forms of AQP3. Densitometric analyses revealed marked decrease in AQP3 expression in the IM in untreated BUO rats compared with SHAM rats. Parecoxib partly prevented this decrease in AQP3 expression in BUO rats. *$P < 0.05$ BUO vs. SHAM. \$ $P < 0.05$ BUO + parecoxib vs. BUO + vehicle. *B–G*: immunohistochemistry for AQP3 in the IM of SHAM, untreated BUO, and parecoxib-treated BUO rats. Immunoperoxidase microscopy demonstrated association of AQP3 labeling with basolateral membranes of principal cells in collecting ducts in the IM of SHAM rats (*B* and *E*). Labeling of AQP3 was reduced in untreated BUO rats (*C* and *F*). Labeling in parecoxib-treated BUO rats was comparable to that in SHAM rats (*D* and *G*).

sion 3 days after release of obstruction ($P < 0.05$; Figs. 9*A* and 10*A*). In kidneys from SHAM rats, immunoperoxidase microscopy demonstrated AQP2 labeling in the apical domains of the IM collecting duct principal cells (Fig. 9, *B* and *E*). In kidneys from BUO rats, AQP2 labeling was less marked (Fig. 9, *C* and *F*) than in SHAM rats. In the obstructed kidneys of parecoxib-treated BUO rats, AQP2 labeling was identical to that in SHAM rats (Fig. 9, *D* and *G*). AQP3 immunoreactivity was associated with the basolateral plasma membrane of the collecting duct principal cells in the IM of the obstructed kidneys (Fig. 10, *C* and *F*), and, similar to AQP2, the labeling was less marked 3 days after release of obstruction than in SHAM rats (Fig. 10, *B* and *E*). AQP3 labeling of the basolateral plasma membrane in the parecoxib-treated rats (Fig. 10, *D* and *G*) was comparable to that in the SHAM rats (Fig. 10, *B* and *E*).

Semiquantitative immunoblotting of pAQP2 was performed using an antibody that selectively recognizes pAQP2, which is phosphorylated at a consensus phosphorylation site for PKA in its COOH terminus (Ser^{256}) (4). The abundance of pAQP2 in the IM was significantly reduced 3 days after release of BUO compared with SHAM rats ($P < 0.01$; Fig. 11*A*) In contrast to AQP2 and AQP3, parecoxib did not change pAQP2 abundance in BUO rats compared with vehicle-infused BUO rats (Fig. 11*A*). In kidney sections from SHAM rats, labeling of pAQP2 was localized to the apical plasma membrane domains of the collecting duct principal cells in the IM (Fig. 11, *B* and *E*). In the obstructed kidney, pAQP2 labeling was significantly weaker and less widely distributed than in SHAM rats (Fig. 11, *C* and *F*). Consistent with findings from immunoblotting, there was no apparent difference in the labeling density of pAQP2 between the parecoxib-treated and untreated BUO rats (Fig. 11, *D* and *G*).

DISCUSSION

The main results of the present study are that COX isoforms change inversely in the prolonged polyuric phase 3 days after release of 24 h of BUO: medullary COX-2 mRNA, protein, tissue distribution, and activity increase in the prolonged polyuric phase, whereas COX-1 mRNA and protein expression decreases. At 3 days after BUO release, a COX-2 inhibitor significantly lowered prostanoid excretion, while polyuria, IM

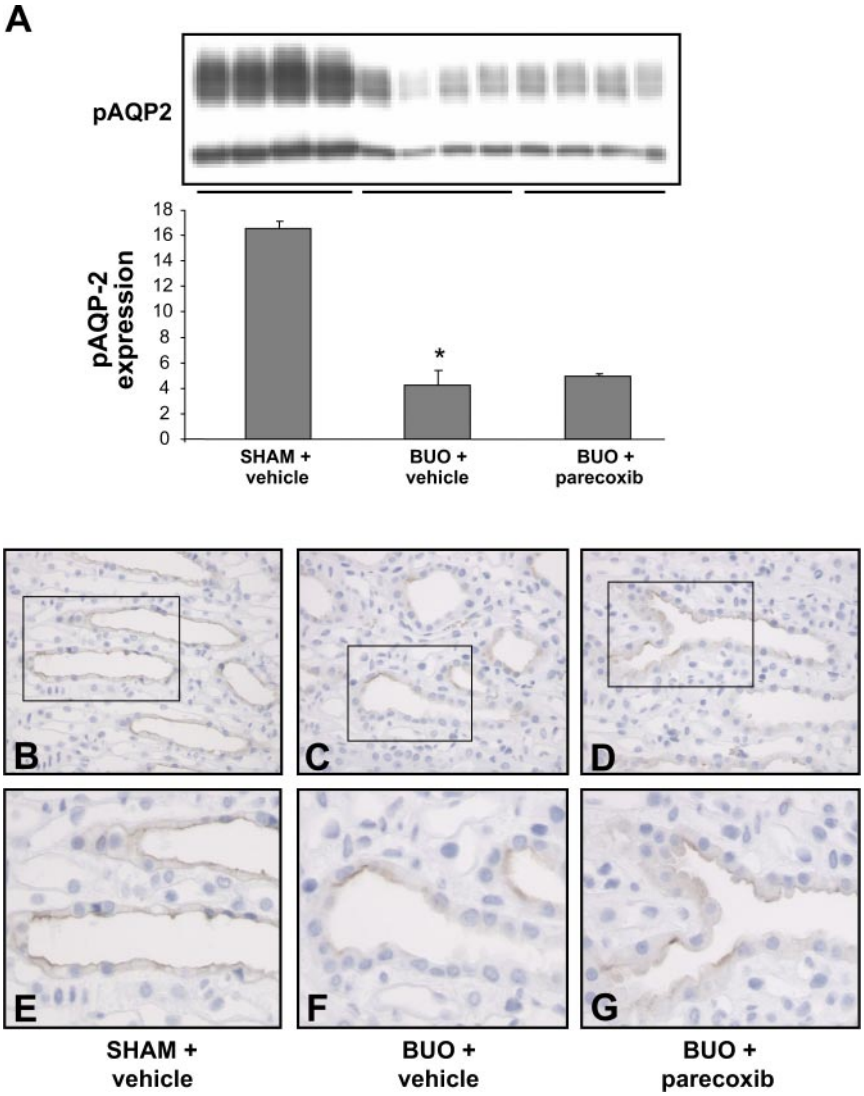

Fig. 11. Semiquantitative immunoblot of phosphorylated AQP2 (pAQP2) in protein isolated from the IM of SHAM, untreated BUO, and parecoxib-treated BUO rats. *A*: immunoblot reacted with affinity-purified anti-pAQP2 antibody. Note 29- and 35- to 50-kDa bands, representing nonglycosylated and glycosylated forms of pAQP2. Densitometric analyses revealed marked decrease in pAQP2 expression in the IM of BUO rats compared with SHAM rats. Parecoxib did not affect decreased pAQP2 expression in BUO rats. $*P < 0.05$ BUO vs. SHAM. *B–G*: immunohistochemistry for pAQP2 in the IM of SHAM, untreated BUO, and parecoxib-treated BUO rats. Immunoperoxidase microscopy demonstrates association of pAQP2 labeling with apical plasma membrane of principal cells in collecting ducts in the IM in SHAM rats (*B* and *E*). Labeling of pAQP2 was reduced in untreated BUO rats (*C* and *F*). Labeling in parecoxib-treated rats was similar to that in nontreated BUO rats (*D* and *G*).

tissue osmolality, and urine-concentrating capacity were the same as in vehicle-treated rats. Furthermore, COX-2 inhibition partially attenuated the reduced expression of AQP2 and AQP3 in medullary collecting ducts. However, the level of NKCC2 mRNA and protein, as well as Na-K-ATPase, in the medullary TAL (mTAL) was unchanged 3 days after release of BUO. Thus COX-2-independent processes are responsible for the increased urine output after release of obstruction. Collapse of the medullary interstitial tissue osmotic gradient appears to be a major factor in the decrease in urine-concentrating capacity.

Inverse regulation of kidney COX-1 and COX-2 after release of obstruction. Previous data show that PGE_2, TxA_2, and prostacyclin synthesis and excretion are increased in UUO and BUO (19). Our present data support the view that COX-2 is responsible for the increase in urinary excretion of PGE_2 and the PGI_2 metabolite 6-keto-$PGF_{1\alpha}$ after release of obstruction. Immunohistochemical staining demonstrated that COX-2 was selectively associated with the medullary interstitial cells 3 days after release of BUO. This pattern of regulation is consistent with the results we and others have demonstrated in previous studies (14, 15, 28, 36). It is well documented that COX-2 expression can be induced by elevated extracellular osmolality in vitro and by water deprivation or AVP infusion in vivo (26). The present study documents a decreased interstitial medullary osmolality in rats 3 days after release of BUO. Thus it is unlikely that the BUO-induced increase in medullary COX-2 expression was directly mediated by changes in tissue osmolality. The present study does not address the mechanisms involved in the medullary induction of COX-2, but several possibilities exist. COX-2 expression is highly regulated by inflammatory mediators. Previous studies have shown that obstruction leads to an intense infiltration of inflammatory cells in the renal interstitium (31).

We observed a significant decrease in COX-1 in kidney IM 3 days after release of obstruction. After 24 h of BUO without release, COX-1 abundance was not affected (28). This difference in responsiveness of COX-1 most likely reflects a turnover rate of expression in the renal medulla that is much slower for COX-1 than for COX-2. Alternatively, factors primarily related to the release phase are responsible for this effect. It has previously been demonstrated that COX-1 expression in the IM was downregulated by chronic lithium treatment (23) and by furosemide administration or water loading in rats (1). Characteristically, these conditions are associated with reduced

renal interstitial osmolality. In cultured IM collecting duct cells, COX-1 mRNA abundance is decreased by exposure of the cells to lower ambient osmolality (1). Collectively, the data are compatible with the notion that the change in interstitial osmolality after release of BUO is a likely signal for the observed decrease in COX-1 expression in kidney IM.

COX-2 inhibition does not prevent polyuria after release of obstruction. Release of BUO is associated with a profound postobstructive polyuria (17, 24), characterized by specific molecular changes of transporters and channels responsible for sodium and water transport in the renal tubules and collecting ducts (12, 22, 24, 25). Previous studies have demonstrated that ureteral obstruction reduces the amounts of luminal Na-K-2Cl cotransporter and basolateral Na-K-ATPase in the mTAL of obstructed kidney and that these reductions contribute to the salt wasting observed after release of obstruction (20). It is well accepted that GFR and renal blood flow are consistently reduced (11, 16, 24), which further supports a tubular origin of the polyuria and renal sodium loss after release of urinary tract obstruction. To examine whether this impairment in urine-concentrating capacity after release of obstruction is regulated by COX-2, we examined the effects of a COX-2 inhibitor during the first 3 days after release of obstruction. Similar to the study of Cheng et al. (2), we observed that COX-2 inhibition significantly reduced urine output only in the acute phase (first 24 h) after release of obstruction. These effects could be mediated by changes in GFR, interstitial or pelvic pressure (29), or transport proteins (28). However, 3 days after release of obstruction, COX-2 inhibition did not alter the profound reduction in renal function. Recently, we demonstrated that selective COX-2 inhibition of rats subjected to 24 h of BUO prevented downregulation of AQP2 and NKCC2 (28). The results of the present study demonstrate that COX-2 inhibition partially prevented downregulation of AQP2 and AQP3. However, the expression of NKCC2 mRNA and protein, as well as Na-K-ATPase, in the mTAL was unchanged 3 days after release of obstruction. A central issue in this apparent controversy is the importance of a potential decrease in collecting duct water permeability relative to the apparent collapse of the interstitial osmotic gradient after 3 days of release. Measurements of interstitial osmolality are technically difficult and depend on the quantitative extraction of osmolytes from the dried tissue and the derivation of tissue blocks from the same level along the cortical-papillary axis. We used a recognized published protocol (33), and the measurements were reproducible. In no case did we observe equilibration between tissue and urine osmolality, and urine osmolality was always much higher than tissue osmolality. These findings are consistent with previous reports and indicate that extraction of osmolytes was not quantitative (28). Nevertheless, interstitial osmolality was always significantly lower in BUO rats. Thus, on the basis of the data, we cannot exclude the possibility that osmotic equilibrium between urine and interstitium is reached when BUO rats are deprived of water and that the major reason for the markedly reduced urine-concentrating capacity is a reduction of interstitial osmolality. The reduced interstitial osmotic gradient in the BUO rats is readily explained by the marked decrease in NKCC2 abundance. This interpretation is also supported by the present results and a previous observation of no improvement in the urine-concentrating capacity, despite a partial prevention in the reduction of AQP2 and AQP3 abundance by parecoxib (24, 25, 28).

PKA activation and phosphorylation of AQP2 are necessary for trafficking of the protein to the apical membrane in the principal cells (5, 13). PGE_2 stimulates removal of AQP2 from the surface of the principal cells when it is added after vasopressin treatment but does not alter the phosphorylated state of AQP2 (38). The present finding that COX-2 inhibition prevents downregulation of AQP2, but not pAQP2, in response to release of obstruction suggests that inhibition of PGE_2 or other PGs leads to a reduction in AQP2 endocytosis and, therefore, increases the abundance of AQP2 in the plasma membrane. However, the total amount of pAQP2 was not increased by COX-2 inhibition, suggesting that sustained phosphorylation may not be required for maintenance of AQP2 in the apical membrane but, rather, that phosphorylation is necessary for translocation of AQP2 from intercellular storage vesicles to the apical membrane, as demonstrated previously (4, 38).

In summary, the present study shows that COX-2 expression is induced in the renal IM, whereas COX-1 expression is reduced, 3 days after release of obstruction. Release of BUO is associated with significant suppression of renal AQPs and renal sodium transporters. Selective COX-2 inhibition partly prevents downregulation of renal IM AQP2 and AQP3 expression but does not affect the medullary protein level of pAQP2 and NKCC2. COX-2 inhibition did not improve urine-concentrating capacity. Thus the present data suggest that changes in bulk AQP2 and AQP3 proteins are less relevant for the diuresis and impaired urine-concentrating mechanism after BUO and that the COX-2-independent, attenuated medullary interstitial osmotic gradient is of major significance in the prolonged polyuric phase of release of BUO.

ACKNOWLEDGMENTS

The authors thank Gitte Kall, Inger Merete Paulsen, Dorte Wulff, Line V. Nielsen, Ida Maria Jalk, and Andreas Rösser for expert technical assistance.

GRANTS

The Water and Salt Research Centre at the University of Aarhus was established and is supported by the Danish National Research Foundation (Danmarks Grundforskningsfond). This study was supported by the Karen Elise Jensen Foundation, the Novo Nordisk Foundation, the WIRED program (Nordic Council and Nordic Centre of Excellence Program in Molecular Medicine), the Danish Medical Research Council, the University of Aarhus Research Foundation, the Danish Cardiovascular Research Academy, the University of Aarhus, the intramural budget of the National Heart, Lung, and Blood Institute, the Kathrine and Vigo Skovgaard Foundation, the Augustinus Foundation, the Beckett Foundation, the LEO Pharma Foundation, the Grosserer L. F. Fogth Foundation, and the A. P. Møller Foundation for the Advancement of Medical Science.

REFERENCES

1. **Castrop H, Vitzthum H, Schumacher K, Schweda F, Kurtz A.** Low tonicity mediates a downregulation of cyclooxygenase-1 expression by furosemide in the rat renal papilla. *J Am Soc Nephrol* 13: 1136–1144, 2002.
2. **Cheng X, Zhang H, Lee HL, Park JM.** Cyclooxygenase-2 inhibitor preserves medullary aquaporin-2 expression and prevents polyuria after ureteral obstruction. *J Urol* 172: 2387–2390, 2004.
3. **Chou SY, Cai H, Pai D, Mansour M, Huynh P.** Regional expression of cyclooxygenase isoforms in the rat kidney in complete unilateral ureteral obstruction. *J Urol* 170: 1403–1408, 2003.
4. **Christensen BM, Zelenina M, Aperia A, Nielsen S.** Localization and regulation of PKA-phosphorylated AQP2 in response to V_2-receptor

agonist/antagonist treatment. *Am J Physiol Renal Physiol* 278: F29–F42, 2000.
5. **Deen PM, Rijss JP, Mulders SM, Errington RJ, van BJ, van Os CH.** Aquaporin-2 transfection of Madin-Darby canine kidney cells reconstitutes vasopressin-regulated transcellular osmotic water transport. *J Am Soc Nephrol* 8: 1493–1501, 1997.
6. **DiGiovanni SR, Nielsen S, Christensen EI, Knepper MA.** Regulation of collecting duct water channel expression by vasopressin in Brattleboro rat. *Proc Natl Acad Sci USA* 91: 8984–8988, 1994.
7. **Earley LE.** Extreme polyuria in obstructive uropathy: report of a case of water-losing nephritis in an infant, with a discussion of polyuria. *N Engl J Med* 255: 600–605, 1956.
8. **Ecelbarger CA, Terris J, Frindt G, Echevarria M, Marples D, Nielsen S, Knepper MA.** Aquaporin-3 water channel localization and regulation in rat kidney. *Am J Physiol Renal Fluid Electrolyte Physiol* 269: F663–F672, 1995.
9. **Ecelbarger CA, Terris J, Hoyer JR, Nielsen S, Wade JB, Knepper MA.** Localization and regulation of the rat renal Na^+-K^+-$2Cl^-$ cotransporter, BSC-1. *Am J Physiol Renal Fluid Electrolyte Physiol* 271: F619–F628, 1996.
10. **Fernandez-Llama P, Ecelbarger CA, Ware JA, Andrews P, Lee AJ, Turner R, Nielsen S, Knepper MA.** Cyclooxygenase inhibitors increase Na-K-2Cl cotransporter abundance in thick ascending limb of Henle's loop. *Am J Physiol Renal Physiol* 277: F219–F226, 1999.
11. **Frokiaer J, Knudsen L, Nielsen AS, Pedersen EB, Djurhuus JC.** Enhanced intrarenal angiotensin II generation in response to obstruction of the pig ureter. *Am J Physiol Renal Fluid Electrolyte Physiol* 263: F527–F533, 1992.
12. **Frokiaer J, Marples D, Knepper MA, Nielsen S.** Bilateral ureteral obstruction downregulates expression of vasopressin-sensitive AQP-2 water channel in rat kidney. *Am J Physiol Renal Fluid Electrolyte Physiol* 270: F657–F668, 1996.
13. **Fushimi K, Sasaki S, Marumo F.** Phosphorylation of serine 256 is required for cAMP-dependent regulatory exocytosis of the aquaporin-2 water channel. *J Biol Chem* 272: 14800–14804, 1997.
14. **Hao CM, Yull F, Blackwell T, Komhoff M, Davis LS, Breyer MD.** Dehydration activates an NF-κB-driven, COX2-dependent survival mechanism in renal medullary interstitial cells. *J Clin Invest* 106: 973–982, 2000.
15. **Harris RC, McKanna JA, Akai Y, Jacobson HR, Dubois RN, Breyer MD.** Cyclooxygenase-2 is associated with the macula densa of rat kidney and increases with salt restriction. *J Clin Invest* 94: 2504–2510, 1994.
16. **Harris RH, Gill JM.** Changes in glomerular filtration rate during complete ureteral obstruction in rats. *Kidney Int* 19: 603–608, 1981.
17. **Harris RH, Yarger WE.** The pathogenesis of post-obstructive diuresis. The role of circulating natriuretic and diuretic factors, including urea. *J Clin Invest* 56: 880–887, 1975.
18. **Hebert RL, Jacobson HR, Breyer MD.** PGE_2 inhibits AVP-induced water flow in cortical collecting ducts by protein kinase C activation. *Am J Physiol Renal Fluid Electrolyte Physiol* 259: F318–F325, 1990.
19. **Himmelstein SI, Coffman TM, Yarger WE, Klotman PE.** Atrial natriuretic peptide-induced changes in renal prostacyclin production in ureteral obstruction. *Am J Physiol Renal Fluid Electrolyte Physiol* 258: F281–F286, 1990.
20. **Hwang SJ, Haas M, Harris HW Jr, Silva P, Yalla S, Sullivan MR, Otuechere G, Kashgarian M, Zeidel ML.** Transport defects of rabbit medullary thick ascending limb cells in obstructive nephropathy. *J Clin Invest* 91: 21–28, 1993.
21. **Kashgarian M, Biemesderfer D, Caplan M, Forbush B 3rd.** Monoclonal antibody to Na,K-ATPase: immunocytochemical localization along nephron segments. *Kidney Int* 28: 899–913, 1985.
22. **Kim SW, Cho SH, Oh BS, Yeum CH, Choi KC, Ahn KY, Lee J.** Diminished renal expression of aquaporin water channels in rats with experimental bilateral ureteral obstruction. *J Am Soc Nephrol* 12: 2019–2028, 2001.
23. **Kotnik P, Nielsen J, Kwon TH, Krzisnik C, Frokiaer J, Nielsen S.** Altered expression of COX-1, COX-2, and mPGEs in rats with nephrogenic and central diabetes insipidus. *Am J Physiol Renal Physiol* 288: F1053–F1068, 2005.
24. **Li C, Wang W, Kwon TH, Isikay L, Wen JG, Marples D, Djurhuus JC, Stockwell A, Knepper MA, Nielsen S, Frokiaer J.** Downregulation of AQP1, -2, and -3 after ureteral obstruction is associated with a long-term urine-concentrating defect. *Am J Physiol Renal Physiol* 281: F163–F171, 2001.
25. **Li C, Wang W, Kwon TH, Knepper MA, Nielsen S, Frokiaer J.** Altered expression of major renal Na transporters in rats with bilateral ureteral obstruction and release of obstruction. *Am J Physiol Renal Physiol* 285: F889–F901, 2003.
26. **Moeckel GW, Zhang L, Fogo AB, Hao CM, Pozzi A, Breyer MD.** COX2 activity promotes organic osmolyte accumulation and adaptation of renal medullary interstitial cells to hypertonic stress. *J Biol Chem* 278: 19352–19357, 2003.
27. **Murer L, Addabbo F, Carmosino M, Procino G, Tamma G, Montini G, Rigamonti W, Zucchetta P, Della VM, Venturini A, Zacchello G, Svelto M, Valenti G.** Selective decrease in urinary aquaporin 2 and increase in prostaglandin E_2 excretion is associated with postobstructive polyuria in human congenital hydronephrosis. *J Am Soc Nephrol* 15: 2705–2712, 2004.
28. **Norregaard R, Jensen BL, Li C, Wang W, Knepper MA, Nielsen S, Frokiaer J.** COX-2 inhibition prevents downregulation of key renal water and sodium transport proteins in response to bilateral ureteral obstruction. *Am J Physiol Renal Physiol* 289: F322–F333, 2005.
29. **Norregaard R, Jensen BL, Topcu SO, Nielsen SS, Walter S, Djurhuus JC, Frokiaer J.** Cyclooxygenase type 2 is increased in obstructed rat and human ureter and contributes to pelvic pressure increase after obstruction. *Kidney Int* 70: 872–881, 2006.
30. **Padi SS, Jain NK, Singh S, Kulkarni SK.** Pharmacological profile of parecoxib: a novel, potent injectable selective cyclooxygenase-2 inhibitor. *Eur J Pharmacol* 491: 69–76, 2004.
31. **Ricardo SD, Ding G, Eufemio M, Diamond JR.** Antioxidant expression in experimental hydronephrosis: role of mechanical stretch and growth factors. *Am J Physiol Renal Physiol* 272: F789–F798, 1997.
32. **Sakairi Y, Jacobson HR, Noland TD, Breyer MD.** Luminal prostaglandin E receptors regulate salt and water transport in rabbit cortical collecting duct. *Am J Physiol Renal Fluid Electrolyte Physiol* 269: F257–F265, 1995.
33. **Schmidt-Nielsen B, Graves B, Roth J.** Water removal and solute additions determining increases in renal medullary osmolality. *Am J Physiol Renal Fluid Electrolyte Physiol* 244: F472–F482, 1983.
34. **Schweer H, Watzer B, Seyberth HW.** Determination of seven prostanoids in 1 ml of urine by gas chromatography-negative ion chemical ionization triple stage quadrupole mass spectrometry. *J Chromatogr* 652: 221–227, 1994.
35. **Sonnenberg H, Wilson DR.** The role of the medullary collecting ducts in postobstructive diuresis. *J Clin Invest* 57: 1564–1574, 1976.
36. **Stubbe J, Jensen BL, Bachmann S, Morsing P, Skott O.** Cyclooxygenase-2 contributes to elevated renin in the early postnatal period in rats. *Am J Physiol Regul Integr Comp Physiol* 284: R1179–R1189, 2003.
37. **Yanagisawa H, Moridaira K, Nodera M, Wada O.** Ureteral obstruction enhances eicosanoid production in cortical and medullary tubules of rat kidneys. *Kidney Blood Press Res* 20: 398–405, 1997.
38. **Zelenina M, Christensen BM, Palmer J, Nairn AC, Nielsen S, Aperia A.** Prostaglandin E_2 interaction with AVP: effects on AQP2 phosphorylation and distribution. *Am J Physiol Renal Physiol* 278: F388–F394, 2000.